Crack Growth Analyses and Correlations for Attachment Lugs

K. Kathiresan*
Lockheed-Georgia Company, Marietta, Georgia
T. R. Brussat†
Lockheed-California Company, Burbank, California
and
J. L. Rudd‡
Air Force Wright Aeronautical Laboratories, Wright-Patterson Air Force Base, Ohio

A method of damage tolerance analysis for corner cracks in attachment lugs is presented and correlated with constant-amplitude fatigue crack growth test results. In the analysis, stress intensity factor solutions for through-the-thickness cracks, obtained from the Green's function method and modified by the use of correction factors, are applied to corner cracks, including transition to a through-the-thickness crack. The accuracy of the analysis is demonstrated through correlations with test results for 24 axially loaded, straight lugs with tiny initial corner cracks. Tests cover three lug shapes, two materials (4340 steel and 7075-T651 aluminum), and two stress ratios, and all tests are replicated.

Nomenclature

a = hole wall crack length of corner crack
a' = imaginary crack length (Fig. 2)
B = thickness of lug
c = surface crack length of corner crack
c_B, c_F = back and front surface crack lengths, respectively (Fig. 2)
c_1, c_2 = two consecutive crack length measurements that bridge the selected 0.025 in. length (or the smallest two measured lengths if all measurements exceed 0.025 in.)
F = hole wall curvature factor
G = Green's (weight) function
K = mode I stress intensity factor
K_C, K_D = stress intensity factors at points C and D, respectively (Fig. 2)
M_B = back surface correction factor
M_c = wall curvature correction factor
M_1'/ϕ = combined front free surface and flaw shape factor
N_1, N_2 = cycle counts for crack lengths c_1 and c_2 in the raw test data
P = total applied pin load
R = stress ratio, $=\sigma_{min}/\sigma_{max}$
R_i = hole (inner) radius of lug
R_o = outer radius of lug
x, y = coordinates perpendicular to and along lug axis, respectively
α = elliptical angle measured from the hole wall
α_t = back surface magnification factor for a transitional crack
β_T = through-the-thickness width correction factor
$\Delta a, \Delta N$ = crack length and load cycle increments
Δa_m = marker cycle crack length increment
ΔN_{eq} = equivalent load cycle increment
ΔN^* = number of cycles added to all raw data values of cycle count to adjust the data to a common initial crack length of 0.025 in.
σ = hoop stress along x axis
σ_{br} = average pin-bearing pressure, $=P/(2R_iB)$
σ_0 = lug gross section stress, $=P/(2R_oB)$
$\bar{\sigma}$ = nondimensional stress, $=\sigma/\sigma_0$

Presented as Paper 83-0842 at the AIAA/ASME/ASCE/AHS 24th Structures, Structural Dynamics and Materials Conference, Lake Tahoe, NV, May 2-4, 1983, received Nov. 12, 1984; revision received May 27, 1985.

*Specialist Engineer. Currently with AT&T Bell Laboratories, Norcross, GA. Senior Member AIAA.
†Staff Scientist.
‡Aerospace Engineer.

Introduction

THE influence of damage tolerance considerations on the structural design, manufacturing, and maintenance of aircraft structures, and the development of nondestructive inspection techniques have been significant over the past decade. In order to assure safety, the U.S. Air Force has imposed damage tolerance requirements in the design of its aircraft.[1] The damage tolerance analysis used in aircraft design requires reliable methods for predicting the growth of a crack from some minimum observable size to the size where unstable growth or fracture is imminent. Such predictions are necessary as a fundamental basis for material selection and stress level control to prevent premature fracture in new designs as well as the establishment of inspection schedules to detect and repair damaged areas before they become critical. To accomplish these predictions, it is necessary to accurately predict stress concentrations, stress intensities, residual strengths, and fatigue crack growth rates in aircraft structures.

Attachment lugs are commonly used for aircraft structural applications. Flaws or cracks can nucleate in attachment lugs due to corrosion, stress corrosion cracking, fretting, tool marks, material defects, and fatigue. The presence of such flaws or cracks elevates the stresses and strains considerably in the vicinity of these imperfections, thus increasing the possibility of abrupt failure or reduction of the lug's operating life. Attachment lugs are particularly critical components from the point of view of crack initiation and crack growth because of their inherently high stress concentration levels near the lug hole. For these reasons, it is important to develop analytical as well as experimental procedures for assessing and designing damage tolerant attachment lugs to ensure aircraft operational safety. Over the years, several extensive studies have been made on lug fatigue performance, involving both experimental and analytical means. Studies of fatigue

characteristics of simple lugs were made by Moon,[2] Schijve and Jacobs,[3] and Edwards and Ryman.[4] Moon[2] also assessed various methods of improving the fatigue life of lugs, and concluded that the methods that offer the greatest potential benefit for practical application are cold working and the use of interference-fit bushings. A method of assessing the effect of an interference-fit bushing on the fracture characteristics of attachment lugs was presented by Hsu and Kathiresan,[5] and recently expanded upon by Kathiresan et al.[6] The effects of cold working, using tapered mandrels and disposable sleeves, on the life of aluminum lugs were summarized by Schijve and Jacobs.[7,8] The fatigue behavior of attachment lugs subjected to other methods of life improvements (such as side relieving of the hole, use of flat-sided pins, lubricant, or surface treatment) has been studied extensively.[9-13]

In the study of fatigue crack growth and fracture behavior of attachment lugs, the essential element is an accurate calculation of the stress intensity factor, K. Over the years several methods have evolved to compute stress intensity factors for structural components containing cracks. These methods include analytical as well as experimental approaches. James and Anderson,[14] for example, used the experimental backtracking approach to empirically derive the stress intensity factors for structural components using growth-rate data of through-the-thickness cracks for simple geometries subjected to constant-amplitude loadings. Analytically, methods have been developed of varying sophistications. A simple compounding method of superposition of known solutions has been applied to lugs by Liu and Kan.[15] Finite element methods in conjunction with special singular crack-tip elements[16-18] have also been used to calculate stress intensity factors. Other methods successfully applied to lug problems are the energy release rate concept[19] and Green's function method.[12] The crack-tip elements were also used to analyze tapered lugs subjected to off-axis and transverse loadings.[20] Most of the preceding investigations are basically two-dimensional in nature, and applicable to through-the-thickness cracks. For the case of a corner crack, which is a three-dimensional problem, several sophisticated methodologies are available. Special three-dimensional crack front elements,[21-23] the alternating method,[24] and the boundary integral equation method[25] can be used to characterize the severity of the singularity along the crack front.

Some fatigue crack growth data have been generated and reported in the literature to support the various proposed analysis methods for through-the-thickness cracks.[6,12,15,19,26,27] However, the published crack growth test data for corner cracks in lugs have been extremely limited.[6,27]

In this paper, the approach adopted by Hsu et al.[28] of modifying the through-the-thickness crack solution with front-free surface, crack shape, curvature, and back surface correction factors has been applied to analyze the corner crack growth in straight attachment lugs. The methodology is verified through correlations with crack growth test results for 24 axially loaded, straight lugs with tiny initial corner cracks. The tests cover three lug shapes, two materials (4340 steel and 7075-T651 aluminum), and two stress ratios, and all tests are replicated.

Analysis Procedure

A corner crack in an attachment lug is more difficult to analyze than a through-the-thickness crack because it has both surface length c and bore depth a; dimensions are shown in Fig. 1. In a rigorous analysis, it should be assumed that the crack grows with different growth rates at all points along the periphery of the crack front. In the present analysis, it is assumed that the crack front shape is a quarter-ellipse and, thus, only the points of intersection of the crack front with the lug surface and the lug hole wall need to be considered. There exists no closed-form analytical solution of stress intensity factors, even for through-the-thickness cracks emanating from a lug hole. To calculate the stress intensity factor solution for a corner crack in an attachment lug, first through-the-thickness crack solutions are obtained for different outer-to-inner radius ratios R_o/R_i and crack lengths c, using the crack-tip finite element method discussed in Ref. 16. In order to enhance the computational efficiency further, a Green's function approach[5] is adopted to calculate the stress intensity factors for through-the-thickness cracks in attachment lugs. The stress intensity factors for through-the-thickness cracks can be calculated using the following equation:

$$K(c) = \sigma_0\sqrt{\pi c}\int_0^1 G(c,\xi)\bar{\sigma}(\xi)\mathrm{d}\xi \tag{1}$$

where $\bar{\sigma} = \sigma/\sigma_0$ is the normalized unflawed stress distribution on the prospective crack surface and $\xi = (x - R_i)/c$ is the nondimensional coordinate. These through-the-thickness crack solutions are then used to estimate the stress intensity factors along the boundary of quarter-elliptical corner cracks in attachment lugs. The procedure is similar to the one developed for fastener holes[28] and is described below.

The stress intensity factor for a single through-the-thickness crack of length c in an attachment lug is given by

$$K(c) = \sigma_0\sqrt{\pi c}\,\beta_T(c/R_i) \tag{2}$$

Then the through-the-thickness stress intensity factor solution is modified by various correction factors to obtain the corresponding stress intensity factor for a single quarter-elliptical corner crack as shown below:

$$K\left(\frac{a}{c},\alpha\right) = \sigma_0\sqrt{\pi a}\,\beta_T\left(\frac{x-R_i}{R_i}\right)\frac{M_1'}{\Phi}\left(\frac{a}{c},\alpha\right) \times M_c\left(\frac{c}{R_i},\frac{x-R_i}{c}\right)M_B\left(\frac{a}{c},\frac{a}{B}\right) \quad \text{for } a/c \le 1 \tag{3}$$

and

$$K\left(\frac{c}{a},\alpha\right) = \sigma_0\sqrt{\pi c}\,\beta_T\left(\frac{x-R_i}{R_i}\right)\frac{M_1'}{\Phi}\left(\frac{c}{a},\alpha\right) \times M_c\left(\frac{c}{R_i},\frac{x-R_i}{c}\right)M_B\left(\frac{a}{c},\frac{a}{B}\right) \quad \text{for } a/c > 1 \tag{4}$$

where

$$M_c = F + \frac{x-R_i}{c}(1-F) \tag{5}$$

and α is the elliptical angle measured from the hole wall, x the distance from the center of the hole to the particular point of interest on the crack periphery, M_1'/Φ the combined front free surface and flaw shape factor, M_c the wall curvature correction factor, M_B the back surface correction factor, and F the hole wall curvature factor. The values of M_1'/Φ and F are presented in Ref. 28. The back surface correction factor, M_B, used in this approach is the one developed and presented in Ref. 29. It is assumed that for a given number of applied load cycles, the extension of the quarter-elliptical crack border is controlled by the stress intensity factors at two points; namely, the intersections of the crack periphery with both the hole wall and the lug surface. In general, the stress intensity factors at these two locations are different, resulting in different crack growth rates. Therefore, the new flaw shape aspect ratio after each crack growth increment differs from the preceding one. The new flaw shape aspect ratio is computed using the new crack lengths at both the hole wall and lug surface.

The preceding process can be repeated until the crack depth a becomes equal to the lug thickness. Then the crack breaks through the back side of the lug and eventually becomes a

through-the-thickness crack, after a transitional crack growth period. This transitional crack growth period was assumed to be negligible in Ref. 28. This assumption is reasonable for a crack at a fastener hole, since the time to grow through the transition region is much smaller than the remaining net section growth period. However, for an attachment lug, when a corner crack grows through the thickness, the remaining net section is usually small in comparison to the surface crack size. Therefore, a proper transitional crack growth criterion is needed for the transition period from the time the crack penetrates the back surface to the time the crack lengths are essentially equal on the front and back surfaces.

Figure 2 shows the transitional crack geometry, in which c_F and c_B are crack lengths on the front and back surfaces, respectively. Collipriest and Ehret[30] proposed a stress intensity magnification factor for the crack tip at the back surface of a surface crack as

$$\alpha_t = \left[1 \Big/ \left\{1 - \sqrt{1 - c_B^2/c_F^2}\right\}\right]^{1/2} \quad \text{for } c_B > 0 \tag{6}$$

It should be noted that when the back side crack length equals the front side crack length, the magnification is unity and the through-the-thickness crack has achieved a uniform front. The above magnification factor is used to calculate the stress intensity factor at the back surface of the transitional crack using the equation

$$K_B = \sigma_0 \sqrt{\pi c_B}\, \beta_T(c_B/R_i)\alpha_t \tag{7}$$

The stress intensity factor at the front surface is calculated using Eq. (4) or (3), assuming an imaginary crack length along the hole wall direction, a', as

$$K_C = \sigma_0 \sqrt{\pi c_F}\, \beta_T\left(\frac{c_F}{R_i}\right) \frac{M_1'}{\Phi}\left(\frac{c_F}{a'}, 90 \text{ deg}\right) M_B\left(\frac{c_F}{a'}, 1\right) \tag{8}$$

The imaginary crack length a' can be determined by fitting the elliptical equation through points C and D as

$$a' = B\{1 - (c_B/c_F)^2\}^{1/2} \tag{9}$$

When the back side crack length c_B approaches that of the front side (i.e., D″C″ as shown in Fig. 2) the factor c_F/a' becomes very small and the corresponding M_1'/Φ ratio approaches unity. After that, the transitional crack becomes a through-the-thickness crack with a uniform front, i.e.,

$$K_D = K_C = \sigma_0 \sqrt{\pi c}\, \beta_T(c/R_i) \tag{10}$$

The stress intensity factors for a growing corner crack in an attachment lug now can be calculated using Eq. (3), (4), (7), (8), or (10), depending upon whether the crack is in the corner, transitional, or through-the-thickness phase.

Equations (3) and (4) were used to generate stress intensity factors for corner cracks in attachment lugs with different aspect ratios, a/c, and geometries, R_o/R_i. Figures 3-5 present the results for R_o/R_i ratios of 1.50, 2.25, and 3.00, respectively. Aspect ratios, a/c, of 1.00, 1.25, and 1.50 were considered and assumed to be constant in each plot. These solutions correspond to corner cracks with $a \leq B$. These part-through crack stress intensity factors are normalized by $\sigma_{br}\sqrt{\pi c}$. Figure 6 presents the normalized stress intensity factors at the lug surface for a constant a/c ratio of 1.33 and an R_o/R_i ratio ranging from 1.50 to 3.00. In this figure, the solutions are presented even after the crack breaks through the back side, i.e., $a > B$.

A computer program[31] was written to calculate crack growth in lugs, using these stress intensity factor solutions in conjunction with a constant-amplitude crack growth-rate curve for the lug material. In the analysis, the corner crack aspect ratio a/c is not held constant but is allowed to vary as the crack grows. After the crack depth a reaches the back surface, the transition behavior is also included. The entire crack growth analysis for a typical lug subjected to constant-

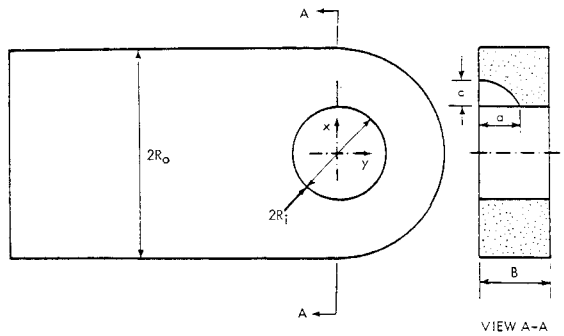

Fig. 1 Geometry of an attachment lug with a corner crack.

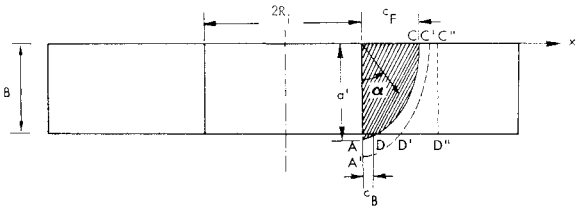

Fig. 2 Transitional crack geometry.

Table 1 Predicted and experimental crack growth lives

Material	R	R_o/R_i	Life, thousands of cycles: Test specimen 1	Test specimen 2	Test geometric mean	Analytical prediction	Life ratios: Test mean / Prediction	Specimen 1 / Specimen 2
Aluminum	0.1	1.5	29.0	28.6	28.8	15.41	1.868	1.01
		2.25	65.8	42.5	52.9	41.52	1.274	1.55
		3.0	63.55	59.09	61.2	57.77	1.059	1.08
	0.5	1.5	139.9	92.0	112.2	51.47	2.180	1.49
		2.25	126.5[a]	57.5[a]	85.3[a]	133.91	0.637[a]	2.20[a]
		3.0	143.4	140.4	141.9	166.87	0.850	1.02
Steel	0.1	1.5	45.5	45.4	45.4	43.81	1.036	1.00
		2.25	99.2	93.3	96.2	108.86	0.884	1.06
		3.0	124.7	114.5	119.5	149.98	0.797	1.09
	0.5	1.5	159.2	146.5	152.7	143.91	1.061	1.09
		2.25	350.8	350.2	350.5	353.39	0.992	1.00
		3.0	476.7	384.5	428.1	486.44	0.880	1.24

[a]Invalid tests: Primary cracking not at electric discharge machined preflaw.

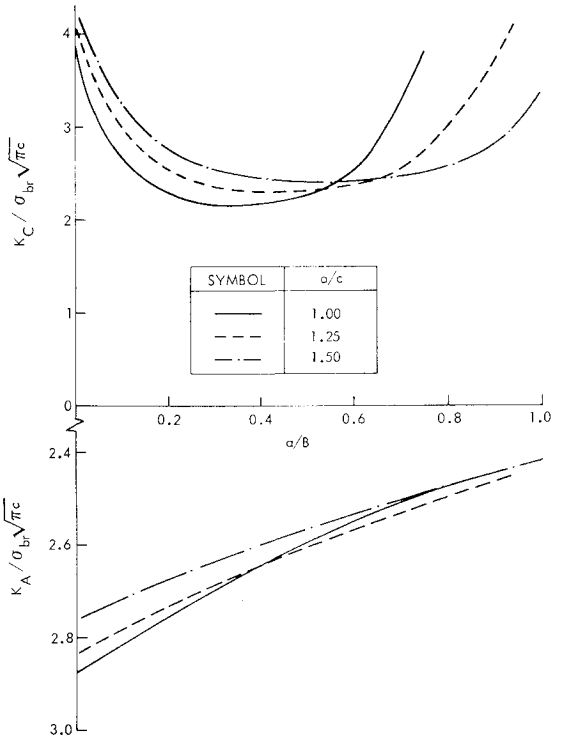

Fig. 3 Normalized stress intensity factors for corner cracks at straight attachment lugs having a R_o/R_i ratio of 1.50 and a B/R_i ratio of 2/3.

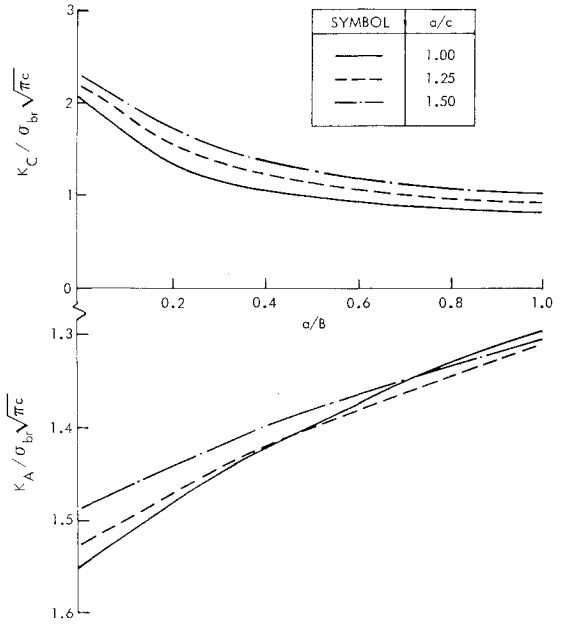

Fig. 4 Normalized stress intensity factors for corner cracks at straight attachment lugs having a R_o/R_i ratio of 2.25 and a B/R_i ratio of 2/3.

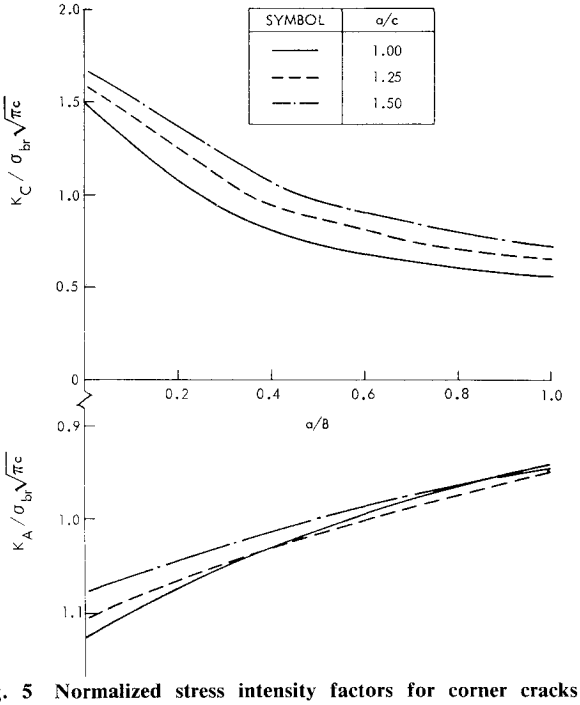

Fig. 5 Normalized stress intensity factors for corner cracks at straight attachment lugs having a R_o/R_i ratio of 3.00 and a B/R_i ratio of 2/3.

amplitude loading can be accomplished within 5 s using the UNIVAC 1100/82 computer.

Test Results and Correlations

Results of 24 constant-amplitude fatigue tests of simple straight-shank attachment lugs with initial corner cracks are presented and correlated with analytical predictions. All tests were replicated, and the testing investigated two materials, two stress ratios ($R = 0.1$ and 0.5), and three values of the lug outer-to-inner radius ratio ($R_o/R_i = 1.50$, 2.25, and 3.0). The two materials, 7075-T651 aluminum and 4340 steel (ultimate tensile strength = 180-200 ksi), were selected based on a survey of attachment lug materials used in aircraft. The survey considered both industry and government sources. A special loading fixture similar to the one used by Schijve and Hoeymakers[27] was designed for the experiments. The loading pin was made of 4340 steel (ultimate tensile strength = 260-280 ksi). The lug inner radius (or the loading pin radius) was kept constant ($R_i = 0.75$ in.) and the outer radius of the lug was varied to obtain the desired R_o/R_i ratio. The thickness of the lugs tested was 0.50 in. Based on the computation of stress concentration factors for these lugs using the finite element method, far-field maximum gross section stresses of 14 and 6 ksi were selected for the steel and aluminum tests, respectively. These selections were made to prevent the maximum peak operating stress from exceeding the yield strength of the materials. These tests were conducted at a cyclic loading frequency of 10 Hz.

For the attachment lug testing, small slots were introduced in the lugs at 90 deg from the load using an electric discharge machine. These slots were approximately 0.01 in. long on the lug surface and the lug hole wall. The specimens were then subjected to fatigue loading to initiate sharp cracks approximately 0.02-0.025 in. long (including the slot). However, sometimes the initial crack lengths were beyond this limit. Thus, for consistency of data presentation, and extrapolation (or interpolation) method was devised to convert the data to a common initial crack length. An initial crack length of 0.025 in. was selected for this purpose, and the cycle count raw data were arithmetically adjusted so that the cycle count for the 0.025 in. crack would be zero. The number of cycles, ΔN^*, to be added to all raw data cycle counts was found by interpolation (or, if necessary, extrapolation) of the raw data. It was observed, in general, that the early crack growth in lugs tended to be approximately linear when plotted as log(c) vs cycles, N. Therefore,

$$\Delta N^* = (N_2 - N_1)\frac{\log(c_2/0.025)}{\log(c_2/c_1)} - N_2 \qquad (11)$$

where c_1 and c_2 are the two consecutive crack length measurements that bridge the 0.025 in. length (or the smallest

two measured lengths if all measurements exceed 0.025 in.) and N_1 and N_2 are the corresponding cycle counts. Note that ΔN^* is always negative if obtained by interpolation and always positive if by extrapolation.

From the initial flaw conditions, testing was continued to lug failure. The crack growth was monitored both by visual measurements with a zoom microscope during testing and the introduction of marker cycle loads for later measurements from photographs of the failure surfaces. The marker cycle loads consisted of constant-amplitude loading with the same test maximum stress level, but a higher stress ratio of 0.85. During data reduction the effects of the marker cycles were accounted for by assuming that the crack growth rate of the marker cycles was the same as the previous constant-amplitude loading. On this basis, an equivalent number of constant-amplitude load cycles was calculated for the marker load cycles as

$$\Delta N_{eq} = \Delta a_m / (\Delta a / \Delta N) \tag{12}$$

where Δa_m is the marker load crack increment, and Δa and ΔN are the previous constant-amplitude crack increment and cycle increment, respectively. These equivalent load cycles were added to the actual constant-amplitude load cycles for each test. Hence the crack growth test data were expressed for a single constant-amplitude load level.

Analytical crack growth calculations were conducted using the stress intensity factors discussed earlier in conjunction with a crack growth-rate curve obtained by testing center-cracked panels. The materials for the center-cracked panels and the lugs came from the same batches. Furthermore, the same stress ratios, $R=0.1$ and 0.5, were used in both sets of tests. Other baseline tests were conducted to obtain fracture toughness and material yield strength for each material. In the analytical predictions for the lugs, it was assumed that the initial 0.025 in. crack had an initial crack aspect ratio, a_0/c_0, of 1.0.

An example of the comparison between experimental and predicted crack growth for duplicate test specimens is shown in Fig. 7. Three crack lengths—front surface crack length c, bore crack length a, and back surface crack length c_B (after the crack breaks through the thickness)—are presented in Fig. 7 as a function of applied constant-amplitude load cycles. The crack lengths c and c_B are presented in the upper half and the crack lengths a are presented in the lower half of the figure. The plotted values of c, shown as open symbols, were obtained visually during the tests. For clarity, not all of the measured values of c are plotted in Fig. 7. The solid line is the analytically predicted growth of crack length c. The plotted values of a and c_B, shown as solid symbols, were obtained from the fractographic examination of marker bands on the fracture surface after each test. The predicted growth of a and c_B is shown as a dashed line. Note that the back surface growth of c_B begins when the crack depth a equals the lug thickness B.

Figure 7 is typical of most of the results. First, it shows very little scatter between the two duplicate test results; the crack growth lives of the two specimens differ by only 9%. Second, the prediction is fairly accurate. The geometric mean crack growth life is 0.8 of the predicted life. Third, the prediction for front surface crack length is fairly accurate, while the prediction for the hole wall crack length is slightly unconservative.

Individual data plots such as Fig. 7 for all 12 test conditions are provided in Ref. 6. As is true of the data shown in Fig. 7, the comparative predicted and actual crack growth lives tend to be excellent measures of both data scatter and accuracy of the prediction. Table 1 summarizes the crack growth life results for all specimens. The column showing the ratio of test lives for the duplicate specimens indicates test scatter. Test results for both of the aluminum lugs with $R_o/R_i=2.25$ and tested at a stress ratio $R=0.5$ are considered invalid because

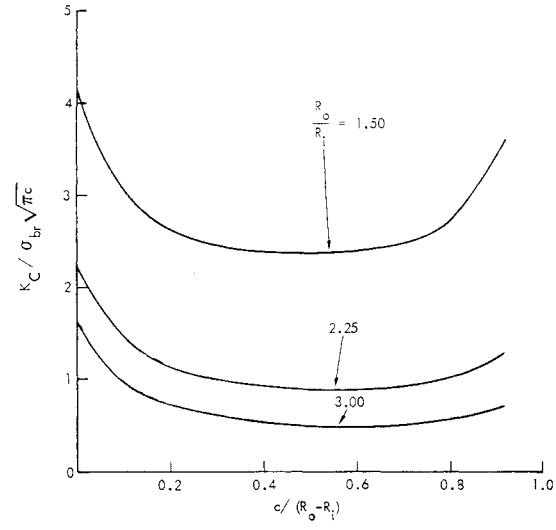

Fig. 6 Normalized stress intensity factors for corner cracks at straight attachment lugs having a constant flaw shape a/c of 1.33.

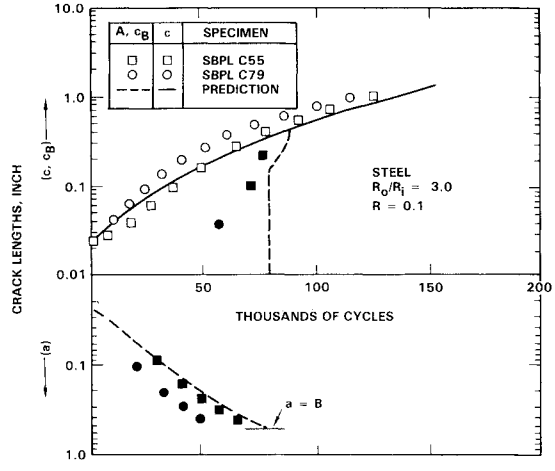

Fig. 7 Typical comparison of crack growth predictions and test results.

final failures were due to the presence and growth of natural cracks and not to the intentional cracks at the machined slots.

Figure 8 summarizes the accuracy of the predicted crack growth lives compared to the corresponding geometric mean test lives. A ratio of 1.0 is a perfect correlation; less than 1.0 is an unconservative prediction; and greater than 1.0 is a conservative prediction. The invalid data point mentioned above is not plotted.

Figure 8 shows that the predictions for the steel specimens were all fairly accurate. However, the predictions for the aluminum specimens ranged from accurate for $R_o/R_i=3.0$ to conservative by a factor of 2.0 for $R_o/R_i=1.5$.

The comparisons of predicted and actual crack growth behaviors of the aluminum specimens with $R_o/R_i=1.5$ are shown in Fig. 9 for $R=0.5$. Whereas the prediction for small cracks is accurate, the crack growth rates are greatly overestimated once crack length c exceeds about 0.1 in. It is this discrepancy that results in the error in predicted life. Essentially the same is true of the $R_o/R_i=1.5$ aluminum specimens tested at $R=0.1$.

Explanations for this isolated discrepancy have been considered, but not investigated in depth. The discrepancy apparently results from synergistic effects involving lug geometry, crack length, and lug material, since it only occurs for aluminum lugs with $R_o/R_i=1.5$ and $c>0.1$ in. The wall

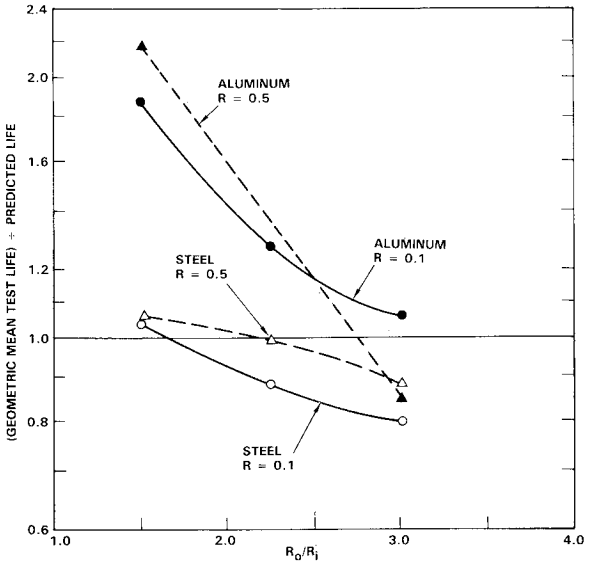

Fig. 8 Accuracy of crack growth life predictions.

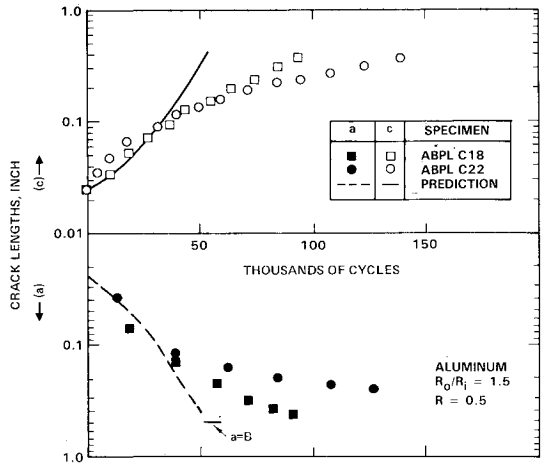

Fig. 9 Conservatism of crack growth predictions for aluminum lugs with $R_o/R_i = 1.5$.

thickness $(R_o - R_i)$ of this particular geometry of lugs is only 25% of the pin diameter. Therefore, there is the possibility of large, geometrically nonlinear deformations, particularly after a significant crack has developed. The analysis was linear and made no allowance for such deformations, if present. In concert with this geometric effect, one of several possible material effects could be influential. For example, since steel pins were used in all cases, the pin-to-lug rigidity ratio for aluminum lugs differs from that of the steel lugs by a factor of 3. Furthermore, the tangential surface tractions between the pin and lug at the crack origin could be considerably different at the aluminum-steel interface than at the steel-steel interface, especially after the differing buildups of fretting debris. Validation of an explanation for the discrepancy would require extensive further work.

Recall that in the analysis method, the crack aspect ratio a/c was not held constant but was allowed to vary as the crack front grew. The stress intensity factors for a growing corner crack were computed using the current aspect ratio a/c. Figure 10 shows typical correlations of analytical/experimental data of corner crack aspect ratios, a/c. The analytical predictions of a/c are poor and can be considered satisfactory at best. Also, there is a large amount of data scatter for duplicate

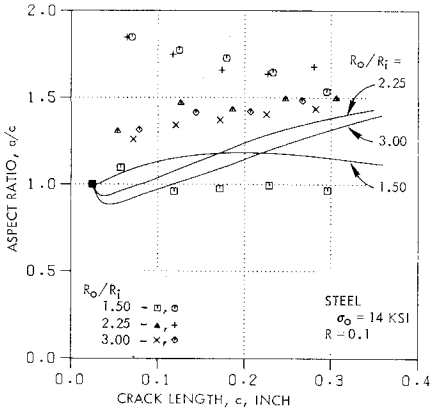

Fig. 10 Typical comparison of measured and predicted crack aspect ratios.

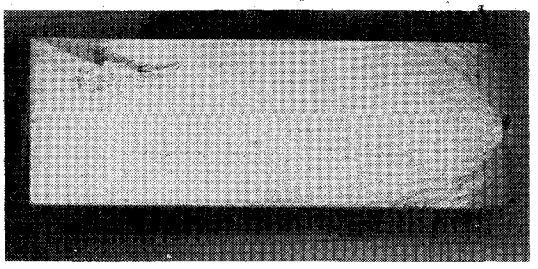

Fig. 11 Fracture surface of a steel lug with marker bands.

tests. This scatter hinders any effort to attempt to improve the analytical predictions.

An example of the fractographic marking capability for the marker cycle technique selected for this program is illustrated in Fig. 11. Very good fractographic markings were obtained for both materials.

Conclusions

A simple analysis procedure for the prediction of corner crack growth behavior in attachment lugs has been developed and presented. In this procedure, the solutions for corner cracks were derived using through-the-thickness crack solutions by modification with various correction factors. The simple and effective Green's function method was employed to compute the through-the-thickness crack solutions. Calculation of corner crack solutions for attachment lugs with the above procedure is extremely cost-effective, as opposed to expensive rigorous three-dimensional procedures. The accuracy of the procedure has been demonstrated in this paper through correlations with experimental results for lugs with various geometries, materials, and stress ratios. Excellent analytical/experimental correlations of the crack growth behavior and life predictions were obtained, except for one case: Crack growth-rate predictions were very conservative for cracks larger than about 0.1 in. in aluminum lugs with $R_o/R_i = 1.50$. This conservatism apparently resulted from some synergistic effects involving variables related to lug geometry, crack length, and lug material. Corner crack aspect ratio predictions were only satisfactory at best.

Acknowledgments

This work was performed under Contract F33615-80-C-3211 for the Flight Dynamics Laboratory, Air Force Wright Aeronautical Laboratories. The authors would like to thank Mr. H.S. Pearson for conducting the experiments reported in this paper.

References

[1]"Airplane Damage Tolerance Requirements," Air Force Aeronautical Systems Div., MIL-A-83444, July 1974.

[2]Moon, J. E., "Improvements in the Fatigue Performance of Pin-Loaded Lugs," Royal Aircraft Establishment Tech. Rept. 80148, Nov. 1980.

[3]Schijve, J. and Jacobs, F. A., "The Fatigue Strength of Aluminum Alloy Lugs," NLR-TR-M2024, ICAF Doc. 99, 1957.

[4]Edwards, P. R. and Ryman, R. J., "Studies in Fretting Under Variable Amplitude Loading Conditions," Royal Aircraft Establishment Tech. Rept. 75132, 1975.

[5]Hsu, T. M. and Kathiresan, K., "Analysis of Cracks at an Attachment Lug Having an Interference-Fit Bushing," *Fracture Mechanics: Fourteenth Symposium,* ASTM STP 791, edited by J. C. Lewis and G. Sines, 1983, pp. I172-I193.

[6]Kathiresan, K. and Brussat, T. R., "Advanced Life Analysis Methods—Experimental Evaluation of Crack Growth Analysis Methods for Attachment Lugs," AFWAL-TR-84-3080, Vol. III, Sept. 1984.

[7]Schijve, J. and Jacobs, F. A., "Programme-Fatigue Tests on Aluminum Alloy Lug Specimens with Slotted Holes and Expanded Holes," NLR-TN-M2139, 1964.

[8]Schijve, J. and Jacobs, F. A., "Comparative Fatigue Tests on Light Alloy Lugs with Normal and Expanded Holes," NLR-TR-68087, ICAF Doc. 441, 1968.

[9]White, D. J., "Effects of Pins with Flats and Resin Bonded Polytetraflourethylene Coating on the Fatigue Strength of Pinned Connections Made from Alloy Steel FV520B," *Proceedings of the Institution of Mechanical Engineers,* Vol. 185, 1970-71, pp. 47-71.

[10]White, D. J., "The Fatigue Strength of Large Single Pinned and Double Pinned Connections Made from Alloy Steel FV520B," *Proceedings of the Institution of Mechanical Engineers,* Vol. 183, Pt. 1, 1968-69, p. 563.

[11]Heber, E., "Fretting Fatigue Strength of Pin Joints in Aluminum Alloys and High Tensile Steel Treated with Various Surface Finishes and Assembled with Various Compounds," Unpublished MOD (PE) material.

[12]Impellizzeri, L. F. and Rich, D. L., "Spectrum Fatigue Crack Growth in Lugs," ASTM STP 595, 1976, pp. 320-336.

[13]Ligenza, S. J., "Cyclic-Stress Reduction within Pin-Loaded Lugs Resulting from Optimum Interference Fits," *Experimental Mechanics,* Vol. 3, 1963, p. 21.

[14]James, L. A. and Anderson, W. E., "A Simple Experimental Procedure for Stress Intensity Factor Calibration," *Engineering Fracture Mechanics*, Vol. 1, 1969, pp. 565-568.

[15]Liu, A. F. and Kan, H. P., "Test and Analysis of Cracked Lugs," *Fracture 1977*, Vol. 3, ICF4, June 1977, pp. 657-664.

[16]Hsu, T. M., "Analysis of Cracks at Attachment Lugs," *Journal of Aircraft,* Vol. 18, Sept. 1981, pp. 755-760.

[17]Pian, T. H. H., Mar, J. W., Orringer, O., and Stalk, G., "Numerical Computation of Stress Intensity Factors for Aircraft Structural Details by the Finite Element Method," AFFDL-TR-76-12, May 1976.

[18]Atluri, S. N., Kobayashi, A. S., and Nakagaki, M., "Application of an Assumed Displacement Hybrid Finite Element Procedure to Two-Dimensional Problems in Fracture Mechanics," *AIAA Journal,* Vol. 13, June 1975, pp. 734-740.

[19]Zatz, I. J., Eidinoff, H. L., and Armen, H., "An Application of the Energy Release Rate Concept to Crack Growth in Attachment Lugs," *Proceedings of the 22nd AIAA/ASME/ASCE Structures, Structural Dynamics and Materials Conference,* Atlanta, GA, April 1981, pp. 402-415.

[20]Kathiresan, K., Hsu, T. M., and Rudd, J. L., "Stress and Fracture Analyses of Tapered Attachment Lugs," *Fracture Mechanics: Fifteenth Symposium,* ASTM STP 833, edited by R. J. Sanford, 1984, pp. 72-92.

[21]Atluri, S. N. and Kathiresan, K., "Stress Analysis of Typical Flaws in Aerospace Structural Components Using Three-Dimensional Hybrid Displacement Finite Element Methods," *Proceedings of the 19th AIAA/ASME/ASCE Structures, Structural Dynamics and Materials Conference*, Bethesda, MD, Aug. 1978, pp. 340-350.

[22]Pian, T. H. H. and Moriya, K., "Three-Dimensional Fracture Analysis by Assumed Stress Hybrid Elements," *Proceedings of the International Conference on Numerical Methods in Fracture*, University College, Swansea, England, Jan. 1978, pp. 363-373.

[23]Raju, I. S. and Newman, J. C. Jr., "Stress Intensity Factors for Two Symmetric Corner Cracks," *Fracture Mechanics,* ASTM STP 677, edited by C. W. Smith, 1979, pp. 411-430.

[24]Nishioka, T. and Atluri, S. N., "Integrity Analysis of Surface-Flawed Aircraft Attachment Lugs: A New, Inexpensive, 3-D Alternating Method," *Proceedings of the 23rd AIAA/ASME/ASCE/AHS Structures, Structural Dynamics and Materials Conference,* New Orleans, LA, May 1982, pp. 287-300.

[25]Heliot, J., Labbens, R., and Pellissier-Tanon, "Application of the Boundary Integral Equation Method to Three-Dimensional Crack Problems," *ASME the Century Two Pressure Vessel and Piping Conference*, Paper 80-C2/PVP-119, San Francisco, CA, Aug. 1980.

[26]Gencoz, O., Goranson, U. G., and Merrill, R. R., "Application of Finite Element Analysis Techniques for Predicting Crack Propagation in Lugs," *Interational Journal of Fatigue*, July 1980, pp. 121-129.

[27]Schijve, J. and Hoeymakers, A. H. W., "Fatigue Crack Growth in Lugs and the Stress Intensity Factor," Delft Univ. of Technology, Delft, the Netherlands, Rept. LR-273, July 1978.

[28]Hsu, T. M., McGee, W. M., and Aberson, J. A., "Extended Study of Flaw Growth at Fastener Holes," AFFDL-TR-77-83, Vol. I, April 1978.

[29]Shah, R. C. and Kobayashi, A. S., "On the Surface Flaw Problem," *The Surface Crack; Physical Problems and Computational Solutions: Proceedings of the ASME Winter Annual Meeting*, edited by J. L. Swedlow, ASME, NY, Nov. 1972, pp. 79-124.

[30]Collipriest, J. E. Jr. and Ehret, R. M., "Computer Modeling of Part-Through Crack Growth," Space Div., Rockwell International Corp., Downey, CA, SD 72-CE-0015B, Oct. 1973.

[31]Kathiresan, K. and Brussat, T. R., "Advanced Life Analysis Methods—User's Manual for 'LUGRO' Computer Program to Predict Crack Growth in Attachment Lugs," AFWAL-TR-84-3080, Vol. VI, Sept. 1984.